

Seismic characterization of slope dynamics caused by softrock-landslides: The Super-Sauze case study

M. Walter & M. Joswig

Institute for Geophysics, Universität Stuttgart, Stuttgart, Germany

ABSTRACT: In this study, we describe the application of *Nanoseismic Monitoring* (Joswig 2008), a seismic ‘microscope’ for small, noisy fracture or impact signals to the Super-Sauze mudslide in the southern French Alps. We were able to detect and locate different signals (type ‘A’ – ‘C’) caused by the movement of the mudslide. Additionally to signals caused by rockfalls in the source area of the slope (type ‘A’), we could identify different types of signals (type ‘B’ and ‘C’), which have been obviously generated by material failure within the unstable part of the mudslide. The spatial distribution of the epicenters (type ‘B’), respectively the estimated source area (type ‘C’), correlates well with parts of the slope moving with higher velocities at the surface. Remarkable is also, that most of these signals have been generated close to the “in-situ crests” (Amirano et al. 2007), which are mostly covered by the mudslide material today. Our preliminary assumption is that the events of type ‘B’ are generated by impulsive fractures within the sliding material, while the events of type ‘C’ are caused by activities at the boundary between the sliding material and the bedrock. We hypothesize that these type ‘C’ events are induced by “scratching” and “grinding” of the moving material against these in-situ crests.

1 INTRODUCTION

1.1 The Super-Sauze mudslide

The mudslide at Super-Sauze is situated in the Barcelonnette Basin in the Southern French Alps, about 100 km north of Nice (Fig. 1). The mudslide started to form in the 1960’s, today it reaches a length of 850 m between 2105 m and 1740 m in elevation. The unstable slope with an estimated volume of 750,000 m³ mainly consists of jurassic, black marls and shows an immense dynamic behaviour with velocities of more than 3 cm.day⁻¹ (Amirano et al. 2007).

1.2 Previous investigations

The mudslide at Super-Sauze has been the target of several investigations since the 1990’s (Weber 1994) in order to develop a comprehensive model for its slope instability. Geological (Weber & Herrmann 2000), hydrological (Malet & Maquaire 2003), geotechnical (Flageollet et al. 1996) and geophysical studies (Schmutz et al. 1999) have been carried out to determine internal structures, the mechanisms as well as the spectrum of influencing and interacting parameters leading to the enormous dynamic of the slope.

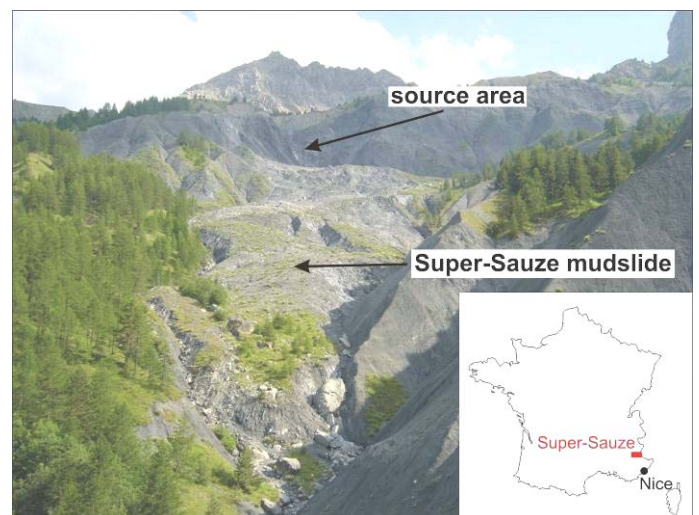


Figure 1. Location of Super-Sauze and upward view of the mudslide and its source area in 2006.

1.3 Seismic monitoring of fracture processes

The seismic monitoring of single fracture processes during the movement of slope instabilities consisting of hard rock (fragments) has been observed by e.g. Spillmann et al. (2007), Roth et al. (2005) and Brückl & Mertl (2006). No fracture processes have been reported from landslides composed of weak sedimentary material. To the best of our knowledge, due to the assumed lack of rigid source areas which could generate sudden material failures, the exis-

tence of such signals hasn't been even expected. Prior work at the Heumoes slope (Walter & Joswig 2008) within the research unit 'Coupling of flow and deformation processes for modeling the movement of natural slopes' (<http://www.grosshang.de>) has demonstrated that the increased sensitivity of the method *Nanoseismic Monitoring* is mandatory to discover local fracture processes in sediments at all. Furthermore, Walter & Joswig (2008) describe the first-time discovery of fractures generated by a landslide consisting of weak sediments.

Comparable to the mudslide at Super-Sauze, the Heumoes slope is set up by loamy scree and glacial till, mostly clayey material with embedded hardrock components of varying size (Lindenmaier et al. 2005). During several field campaigns within the last three years, we were able to detect and locate single fracture processes accompanying the movement of the Heumoes slope. The spatial distribution of the located epicenters correlates to parts of the slope showing higher movement velocities at the surface (Walter & Joswig 2008). The temporal occurrence of these events indicates a rainfall-triggered stress relief within the sliding body, potentially caused by fast subsurface water dynamics.

According to these results and to the fact that the mudslide at Super-Sauze consists of comparable weak sediments, we applied the method *Nanoseismic Monitoring* to Super-Sauze in order to detect and locate possible seismic signals caused by material failure during its movement.

2 DATA ACQUISITION/DATA PROCESSING

Seismic data was acquired during a 10-day campaign (14th – 24th of July 2008) by deploying four tripartite seismic mini arrays on the Super-Sauze mudslide (Fig. 4). Each Seismic Navigating System (SNS) consists of one 3c and three 1c short period seismometers with an aperture of 20-25 m. Data was recorded in continuous mode by different dataloggers, set to a sampling rate of 400 (500) Hz.

The data was processed using the software HypoLine, an interactive, graphical jackknife tool which displays the most plausible solution for low-SNR (signal to noise ratio) signals, resolving the influence of individual parameters on the location of events in real-time (Joswig 2008).

The raw-data was high-pass filtered above 5 Hz to eliminate anthropogenic noise sources and to increase SNR. A ~10 times higher anthropogenic noise-level during daytime has been caused mainly by colleagues who worked all over the slope during the whole field campaign.

3 CALIBRATION SHOT ANALYSIS

To determine an adequate underground model for the localization of possible slope dynamics, we ignited 8 calibration shots on several locations of the slope, close to our stations. We determined a P- and S-wave velocity of about 600 m/s and 310 m/s within the unstable sediments, respectively. For the bedrock below, we determined a P-wave velocity of about 2100 m/s and S-wave velocity of 1200 m/s.

The considerable low phase velocities as well as the lower v_P/v_S ratio of the unstable material compared to the bedrock below is quite common for sedimentary bodies (e.g. Walter & Joswig 2008) and in accordance with prior seismic investigations at Super-Sauze (Grandjean et al. 2007). The relatively low P-wave velocity of the bedrock below is also consistent with the ones observed at the mudslide in previous studies. Grandjean et al. (2007) determined a P-wave velocity between 2100 m/s and 2400 m/s. Thus, we used a layer above halfspace model with the mentioned phase velocities for further event localization, if possible.

4 SEISMIC MONITORING OF SLOPE DYNAMICS

During the measurement period we were able to detect and locate different types of events caused by material failure within the source area and the mudslide itself (Fig. 1). The types differ in duration, amplitude, frequency content and consequently in sonogram patterns. These characteristics as well as the analysis of further site-effects, like amplitude decrease, absorption and attenuation effects, allowed us to distinguish the events. Generally, we identified three types of events (type 'A' – 'C') on the basis of the mentioned attributes, which will be discussed additionally (Tab. 1).

Table 1. Classification criteria of recorded event types.

Classification criteria	type 'A'	type 'B'	type 'C'	type 'C*'
Signal duration	sec.-min.	2-5 sec.	2-20 sec.	< 2 sec.
Frequency content	10-130 Hz	10-80 Hz	5-150 Hz	5-150 Hz
Stations	2-4 SNSs	1-3 SNSs	1 SNS	1 station
Amplitude [nm/s]	80-1500	40-200	100-7500	20-60

4.1 Event type 'A'

During the field campaign, we recorded hundreds of signals with durations between a few seconds (single event) and up to 20 minutes (multiple events). The signals show a high-frequented 'noise band' up to ~130 Hz with broadband spikes (Fig. 2). The maximum amplitude (peak to peak) of these events varies between 80 nm.s⁻¹ and 1500 m.s⁻¹. The weaker ones were recorded at only two, the stronger ones at all four SNSs.

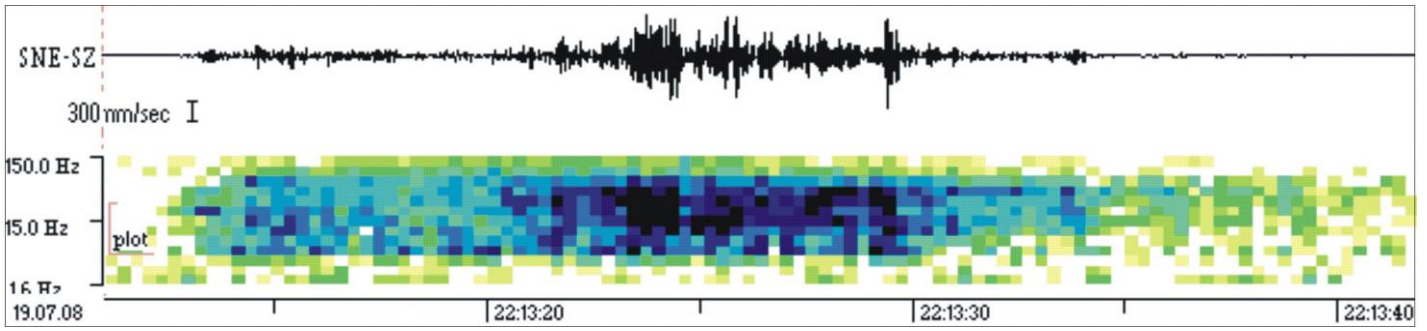


Figure 2. Typical waveform and sonogram pattern of one event of type 'A', recorded with the closest 1c station in ~50 m distance.

The source area of the type 'A' events has been estimated by the determination of the backazimuth with each SNS. All these events of type 'A' occurred in the steep, North-facing hillsides, on the brink of the most upper part of the mudslide.

4.2 Event type 'B'

During the field campaign we could record, identify and locate 34 events of type 'B', which show remarkable differences to the events type 'A'. The signals of type 'B' events show clear P- and S-wave onsets, allowing their localization (Fig. 3).

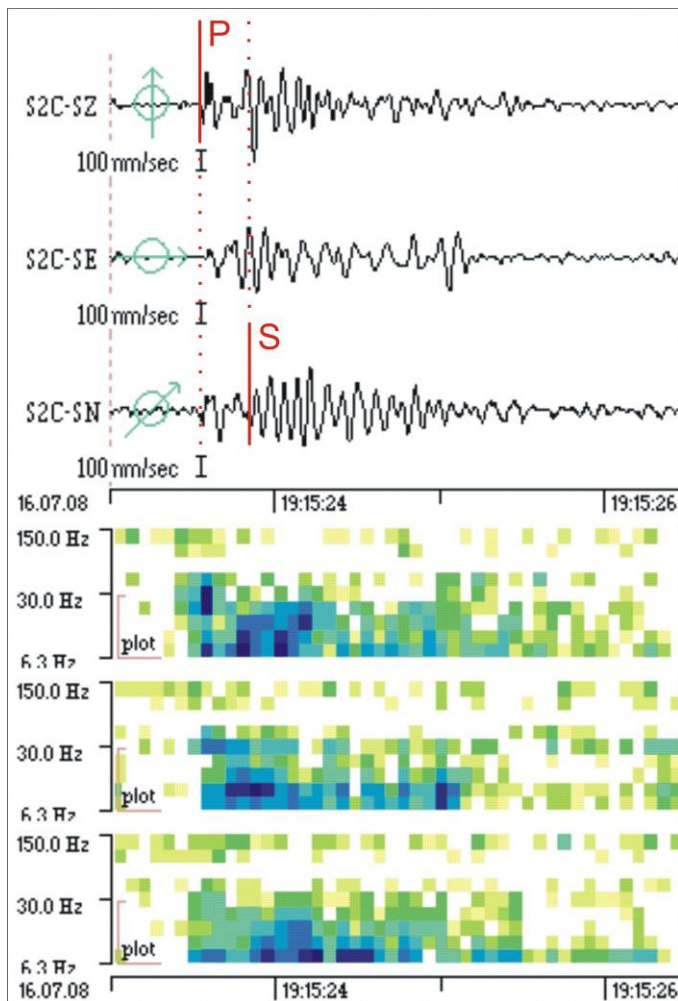


Figure 3. Typical waveforms and sonogram patterns of one event of type 'B', $M_L = -2.2$ in ~120 m distance, recorded with a 3c-station, and the determined phase onsets (red).

The duration of these signals is 2-5 seconds; the maximum amplitude (peak to peak) varies between 40 and 200 nm/s. Consequently, only a few of these events were recorded at all four SNSs. To locate them, the events had to be recorded at least at two SNSs. Due to the short epicentral distances; the different wave phases can hardly be separated. In contrast to the P-phase, the later arriving wave phases can't be separated from each other, which is indeed redundant for event localization. The onset of a mixed coda of S- and surface waves with a velocity of ~300 m/s, which is quite similar to the S-wave velocity within the unstable material determined with the calibration shots, could be identified (Fig. 3). Caused by the relatively low S-wave velocity of 310 m/s and probably superficial source mechanisms, surface waves are present in the coda.

The signal energy of these events concentrates in higher frequency P-phases with 10-80 Hz than the later arriving phases with 10-30 Hz (Fig. 3). The emergent onset, the lack of high frequencies above 80 Hz and the incoherency of the signals are typical for the intense scattering of signal energy caused by the high heterogeneity of the slope material. The determined magnitudes of these type 'B' events vary between $-3.2 \leq M_L \leq -1.3$.

The located fractures are mainly clustered in the mid part of the mudslide (Fig. 4), correlating with the part of the slope showing the highest velocities at the surface. The three events located in the south, outside of the slope catchments, are probably generated by material failure in the hard rock mass in the source area of the mudslide. Remarkable is, that a cluster of these type 'B' events is located directly at the boundary between the mudslide material and one of the emerging in-situ crests in the mid part of the slope (Fig. 4).

The estimated detection threshold for the events of type 'B' is $M_L = -2.6$ for a slant distance of about 140 m. The weakest event of $M_L = -3.2$ has been recorded in a distance of ~70 m, the strongest one of $M_L = -1.3$ in ~200 m distance to the closest station. The estimated location accuracy is about 10 % of the epicentral distance. As the event depth could not be evaluated due to the sparse station distribution, it is neither impossible to estimate at which depth nor along which material interface the source processes took place exactly.

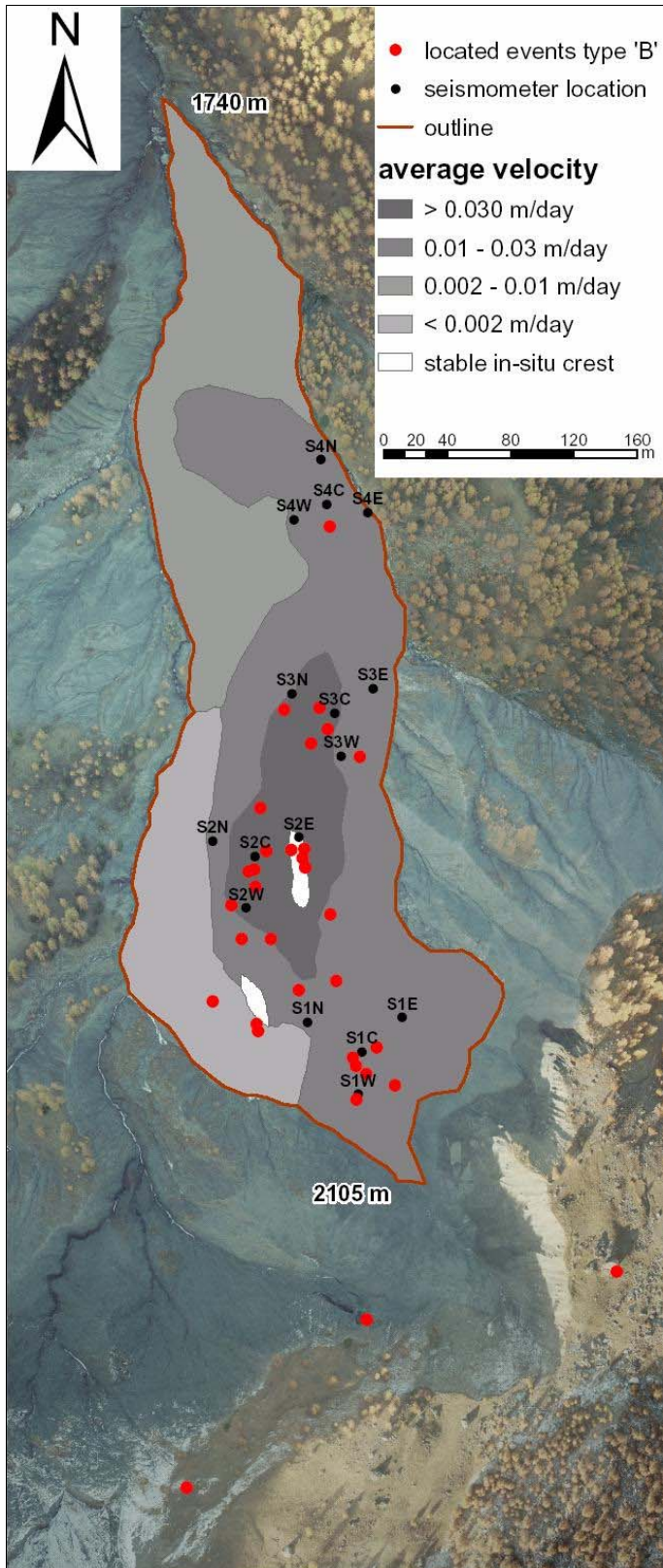


Figure 4. Location of the installed seismometer stations (black dots), epicenters of the located events of type 'B' (red dots) and average movement velocity of the mudslide (1997-2007) mapped on a LIDAR scan (2007).

The temporal occurrence of the type 'B' events, their magnitudes and the rain intensity during the field campaign is displayed in Figure 5. It seems that the mudslide moves more or less continuously, indicated by the distributed temporal occurrence of the

signals all over the measurement period. Note, that a cluster of events with the highest magnitudes occurred just a few hours after the rain event on 21st of July 2008.

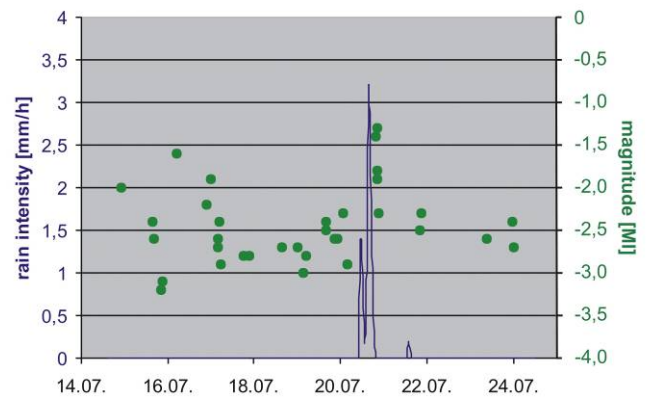


Figure 5. Rain intensity (blue) and temporal occurrence of the type 'B' events with their magnitudes M_L (green) during the field campaign 14th -24th of July 2008.

4.3 Event type 'C'

Beside the events of type 'A' and type 'B', we recorded and identified 44 signals showing significant differences. The duration of these events of type 'C', which were only recorded at one single SNS, varies between 2-20 seconds. Compared to the other event types, the signal energy is prevailing at higher frequencies up to 150 Hz at the closest station in the array (Fig. 6). Due to the heterogeneity of the slope material, we see enormous attenuation effects within one single SNS; the signal amplitude decreases about 30 times within one single SNS at the same time (Fig. 6).

Similar to the events of type 'A', no wave phases could be identified, which disallowed their localization. Therefore we could only estimate the source area, which is for obvious reasons, in the vicinity of the closest station with the highest recorded amplitude.

Figure 7 shows the stations where we determined the source area of the recorded events of type 'C' with the amount of them during the whole field campaign. Like the type 'B' event locations, most of the type 'C' events occurred in the mid part of the slope. The source area of 64 % of these events is estimated to be close to the station S2E, at the boundary of the slope material and one of the emerging in-situ crests as well.

Hundreds of much weaker events showing a similar frequency content have been recorded at only one single station (Fig. 8). The signals lie barely above the natural noise-level and could only be identified by sonogram analysis.

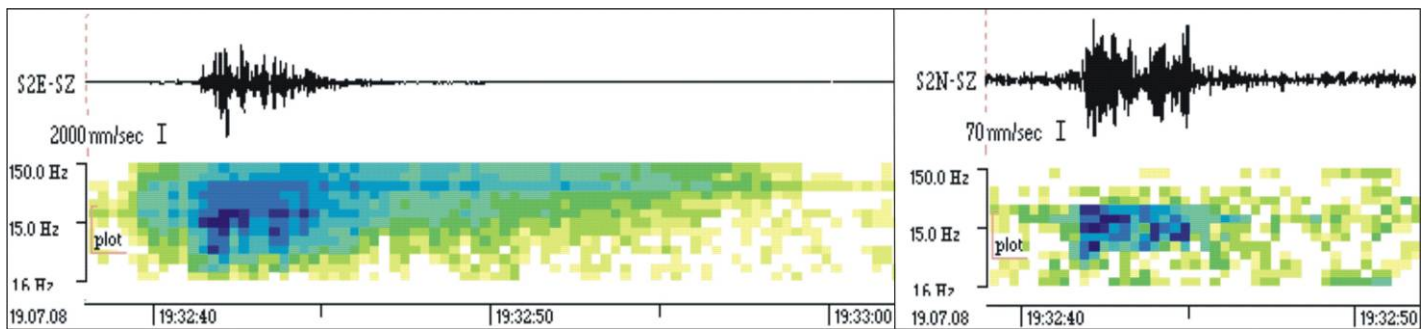


Figure 6. Typical waveforms and sonogram patterns of one event of type 'C', recorded with a 1c-station close to the source location (left) and with a 1c-station in a distance of ~25m (right).

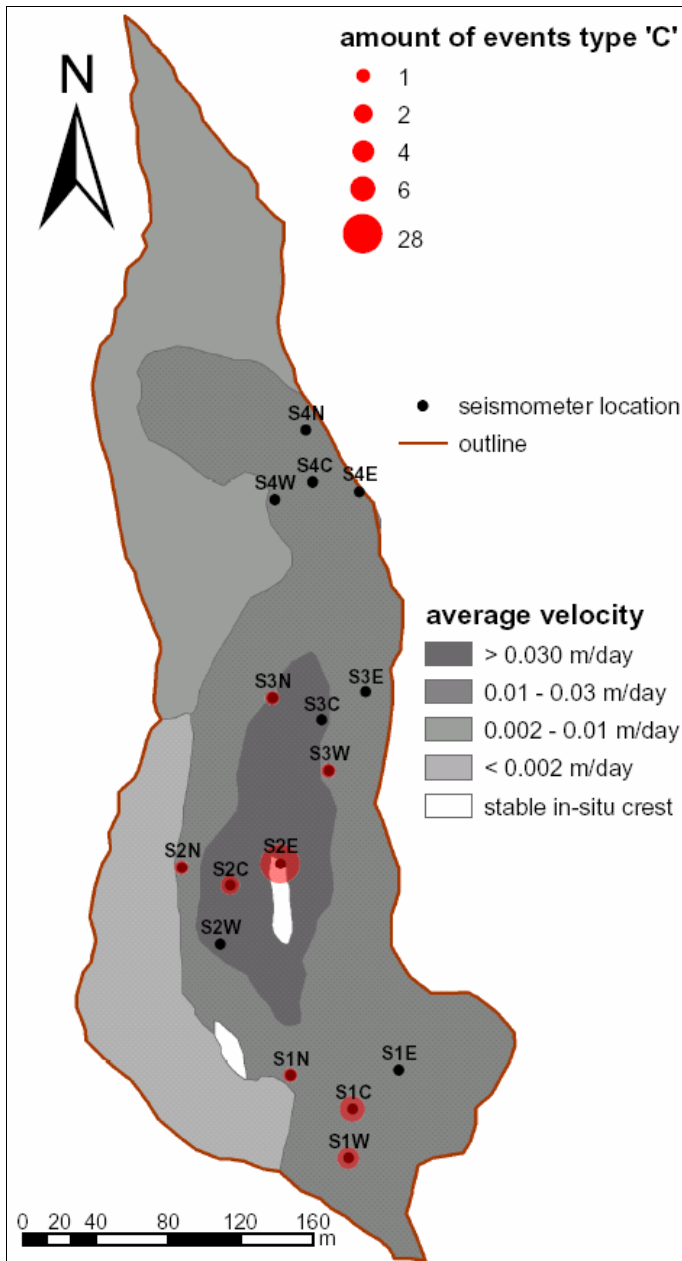


Figure 7. Location of the installed seismometer stations (black dots) with the amount of the events of type 'C' generated close to them (red) and average movement velocity of the mudslide (1997-2007).

The duration of these signals is less than two seconds; the energy is dominated by higher frequencies up to 150 Hz (Fig. 8).

Consequently, these signals have been classified as weak type 'C' events, termed as events type 'C*' (Tab. 1). The only difference to the mentioned type

'C' events is the downscaled amplitude and signal duration. These events occurred nearly all over the slope, but most of them, again, close to the station S2E at the boundary between the sliding material and one of the emerging in-situ crests.

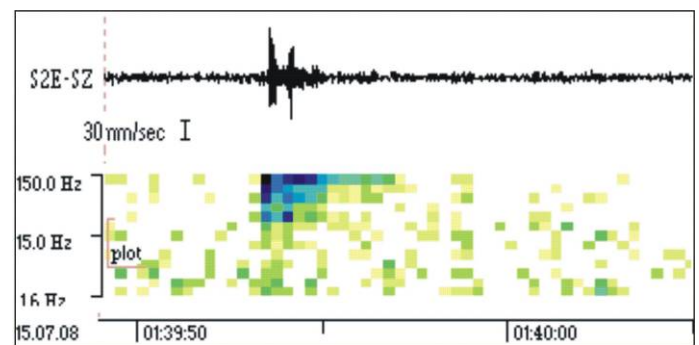


Figure 8. Waveform and sonogram of one event of type 'C*', recorded with one single 1c-station in a few meters distance.

5 CONCLUSIONS

Applying the method *Nanoseismic Monitoring* we were able to detect and partly locate distinct types of events caused by the dynamics at the Super-Sauze mudslide. Waveform and sonogram analysis were applied to discriminate the event types.

As the signals of events of type 'A' are generally similar to those of avalanches (e.g. Suriñach et al. 2005), we interpret the events of type 'A' as signals caused by rockfalls. The broadband spikes in the signals are generated by falling blocks, which has been proved by field experiments. The source area of the events of type 'A' is estimated to be at the upper most part of the slope, where rockfalls with components of varying size occur frequently.

The wave phases of the signals of the events of type 'B' could be identified, which allowed their localization. The spatial distribution of the epicenters of the type 'B' events correlates quite well with parts of the slope showing the highest movement velocities. The highest magnitudes of these events have been observed a few hours after a rainfall event on 21st of July 2008. Except that, the temporal occurrence of these type 'B' events is more or less statistically distributed without any tendencies over the whole measurement period.

That means, that the slide obviously relieves stress continuously, but extensive rainfall can trigger stronger material failure processes. The influence of rain events to the stability of landslides consisting of weak sediments has been seismically observed at the Heumoes slope as well (Walter & Joswig 2008). Up to now we assume, that fracture processes within weak sediment material in general, can be generated in dependence of its water saturation. Shear strength analysis of the material of the mudslide at Super-Sauze in dependence of its water saturation showed the highest values between 12-15 % water content (Malet 2003). These values are consistent to those of the first few meters under the surface of the slope. Below, the material is more or less water saturated. Hence, we presume that the events of type 'B' are generated close to the surface within the sliding material. This hypothesis is also based on the observed presence of surface waves in the signal coda.

The fact, that we located most of the events of type 'B' directly at the boundary between the sliding material and one of the emerging in-situ crests suggests the possibility of higher stress relief at that boundary in general. To proof this assumption, we overlaid the location of all these events with an airborne picture taken in 1956, before the mudslide occurred. Most of the epicenters are mainly located on top of the in-situ crests, today hidden by the mudslide material.

Our actual hypothesis is that the events type 'B' are generated by impulsive fractures within the sliding material while the events of type 'C' are caused by activities at the boundary between the sliding material and the bedrock. We assume that these events of type 'C' are induced by "scratching" and "grinding" of the moving material against the, mostly covered, in-situ crests. To corroborate this hypothesis and to determine the exact source mechanisms, further research has to be done.

ACKNOWLEDGEMENTS

We thank Jean-Philippe Malet for both, providing the LIDAR scan from 2007 (Figure 4) and several airborne pictures which helped enormous to analyze our data, and for the very helpful discussions. We also thank all the colleagues who joined and supported us at the mudslide in Super-Sauze in July 2008. The authors are grateful to the reviewer Denis Jongmans for his improvements of the manuscript.

REFERENCES

Amitrano, D., Gaffet, S., Malet, J.-P. & Maquaire, O. 2007. Understanding mudslides through micro-seismic monitoring: the Super-Sauze (South-East French Alps) case study. *Bulletin de la Société Géologique de France* 178 (2) : 149-157.

Brückl, E. & Mertil, S. 2006. Seismic Monitoring of Deep-Seated Mass Movements. *Proc. INTERPRAEVENT: Inter-*

national Symposium "Disaster Mitigation of Debris Flows, Slope Failures and Landslides." Universal Academy Press, Inc. / Tokyo, Japan: 571-580.

Flageollet, J.C., Maquaire, O. & Weber, D. 1996. Geotechnical investigations into the Super-Sauze landslide. Geomorphological and hydrogeological results. In: *Workshop: 'Landslides-Flash floods' Barcelonnette-Vaison la Romaine*, CERG, European Council: 30-38.

Grandjean, G., Malet, J.-P., Bitri, A. & Méric, O. 2007. Geophysical data fusion by fuzzy logic for imaging the mechanical behaviour of mudslides. *Bulletin de la Société Géologique de France* 178 (2): 127-136.

Joswig, M. 1990. Pattern recognition for earthquake detection. *Bull. seism. Soc. Am.* 80: 170-186.

Joswig, M. 2008. Nanoseismic Monitoring fills the gap between microseismic networks and passive seismic, *First Break* 65: 121-128.

Lindenmaier, F., Zehe, E., Dittfurth, A. & Ihringer, J. 2005. Process identification at a slow-moving landslide in the Vorarlberg Alps, *Hydrological Processes* 19: 1635-1651.

Malet, J.-P. 2003. *Les glissements de type écoulement dans les marnes noires des Alpes du Sud. Morphologie, fonctionnement et modélisation hydro-mécanique*. Phd thesis, Université Louis Pasteur, Strasbourg: 364p.

Malet, J.-P. & Maquaire, O. 2003. Hydrological behaviour of earthflows developed in clay-shales: investigation, concept and modelling. In Picarelli, L. (Ed): *The Occurrence and Mechanisms of Flows in Natural Slopes and Earthfills*, Patron Editore, Bologna: 175-193.

Roth, M., Dietrich, M., Blikra, L.H. & Lecomte, I. 2005. Seismic monitoring of the unstable rock slope at Åknes, Norway. *NORSAR*, Report for the International Centre for Geohazards.

Schmutz, M., Guérin, R., Maquaire, O., Desclôitres, M., Schott, J.-J. & Albouy, Y. 1999. Contribution of a combined TDEM (Time-Domain Electromagnetism) and electrical survey to the investigation of the super sauze flow-slide internal structure. *Comptes Rendus de l'Académie de Sciences - Serie IIa: Sciences de la Terre et des Planetes*, 328 (12) : 797-800.

Spillmann, T., Maurer, H., Green, A. G., Heincke, B., Willenberg, H. & Husen, S. 2007. Microseismic investigations of an unstable mountain slope in the Swiss Alps. *J. Geophys. Res.* 112 B07301.

Suriñach, E., Vilajosana, I., Khazaradze, G., Biescas, B., Furdada, G. & Vilaplana, J.M. 2005. Seismic detection and characterization of landslides and other mass movements. *Nat. Hazards Earth Syst. Sci.* 5: 791-798.

Walter, M. & Joswig, M. 2008. Seismic monitoring of fracture processes generated by a creeping landslide in the Vorarlberg Alps, *First Break* 65: 131-135.

Weber, D. 1994. Research into earth movements in the Barcelonnette basin. In Casale, R., Fantechi, R., Flageollet, J.C. (Eds): *Temporal occurrence and forecasting of landslides in the European Community, Final report, Volume I.*, Contract EPOCH, European Commission: 321-336.

Weber, D. & Herrmann, A. 2000. Reconstitution de l'évolution géomorphologique de versants instables par photogrammétrie numérique : l'exemple du glissement de terrain de Super-Sauze (Alpes-de-Haute-Provence, France). *Bulletin de la Société Géologique de France* 171: 637-648